STEM CELLS®

TISSUE-SPECIFIC STEM CELLS

Multipotent Neural Stem Cells from the Adult Tegmentum with Dopaminergic Potential Develop Essential Properties of Functional Neurons

ANDREAS HERMANN,[a,b,c] MARTINA MAISEL,[a,c] FLORIAN WEGNER,[d] STEFAN LIEBAU,[a,e] DONG-WOOK KIM,[b] MANFRED GERLACH,[f] JOHANNES SCHWARZ,[d,g] KWANG-SOO KIM,[b] ALEXANDER STORCH[c]

[a]Department of Neurology, University of Ulm, Ulm, Germany; [b]Molecular Neurobiology Laboratories; McLean Hospital/Harvard Medical School, Belmont, Massachusetts, USA; [c]Department of Neurology, Technical University of Dresden, Dresden, Germany; [d]Department of Neurology, University of Leipzig, Leipzig, Germany; [e]Department of Anatomy and Cell Biology, University of Ulm, Ulm, Germany; [f]Clinical Neurochemistry, Department of Child and Youth Psychiatry and Psychotherapy, University of Würzburg, Würzburg, Germany; [g]Division of Biology, California Institute of Technology, Pasadena, California, USA

Key Words. Adult neurogenesis • Neural stem cells • Dopaminergic differentiation • Parkinson's disease • Electrophysiology Neuroregeneration

ABSTRACT

Neurogenesis in the adult brain occurs within the two principal neurogenic regions: the hippocampus and the subventricular zone of the lateral ventricles. The occurrence of adult neurogenesis in non-neurogenic regions, including the midbrain, remains controversial, but isolation of neural stem cells (NSCs) from several parts of the adult brain, including the substantia nigra, has been reported. Nevertheless, it is unclear whether adult NSCs do have the capacity to produce functional dopaminergic neurons, the cell type lost in Parkinson's disease. Here, we describe the isolation, expansion, and in vitro characterization of adult mouse tegmental NSCs (tNSCs) and their differentiation into functional nerve cells, including dopaminergic neurons. These tNSCs showed neurosphere formation and expressed high levels of early neuroectodermal markers, such as the proneural genes *NeuroD1*, *Neurog2*, and *Olig2*, the NSC markers Nestin and Musashi1, and the proliferation markers Ki67 and BrdU (5-bromo-2-deoxyuridine). The cells showed typical propidium iodide–fluorescence-activated cell sorting analysis of slowly dividing cells. In the presence of selected growth factors, tNSCs differentiated into astroglia, oligodendroglia, and neurons expressing markers for cholinergic, GABAergic, and glutamatergic cells. Electrophysiological analyses revealed functional properties of mature nerve cells, such as tetrodotoxin-sensitive sodium channels, action potentials, as well as currents induced by GABA (γ-aminobutyric acid), glutamate, and NMDA (*N*-methyl-d-aspartate). Clonal analysis demonstrated that individual NSCs retain the capacity to generate both glia and neurons. After a multistep differentiation protocol using co-culture conditions with PA6 stromal cells, a small number of cells acquired morphological and functional properties of dopaminergic neurons in culture. Here, we demonstrate the existence of adult tNSCs with functional neurogenic and dopaminergic potential, a prerequisite for future endogenous cell replacement strategies in Parkinson's disease. STEM CELLS *2006;24:949–964*

INTRODUCTION

Neurogenesis in the adult mammalian brain is a generally accepted phenomenon in two discrete neurogenic regions: the hippocampus and the subventricular zone (SVZ) of the lateral ventricles [1–5]. In recent years, neurogenesis was reported to occur in other regions of the adult brain under normal conditions, such as the neocortex [2], amygdala [6], and substantia nigra [7]. Moreover, various brain insults have been shown to induce the production of new neurons in the striatum [8], cortex [9, 10], and substantia nigra [7]. However, other research groups were not able to replicate some of these reports [11, 12], and some have been challenged on methodological grounds [11–15].

Correspondence: Alexander Storch, M.D., Technical University of Dresden, Department of Neurology, Fetscherstrasse 74, 01307 Dresden, Germany. Telephone: +49-351-458-2532; Fax: +49-351-458-4352; e-mail: alexander.storch@neuro.med.tu-dresden.de
Received April 26, 2005; accepted for publication December 9, 2005; first published online in STEM CELLS *EXPRESS* December 22, 2005. 1066-5099/2006/$20.00/0 doi: 10.1634/stemcells.2005-0192

For example, a recent study by Frielingsdorf and colleagues [13] could not reproduce the data reported by Zhao and coworkers [7] showing adult dopaminergic neurogenesis in the substantia nigra, including re-establishment of the nigro-striatal dopaminergic connections. They did not find newly generated dopaminergic neurons by the 5-bromo-2-deoxyuridine (BrdU) incorporation assay in normal or 6-hydroxydopamine–lesioned animals. They further argued that in vivo labeling of new neurons in the substantia nigra with DiI might be related to retrograde labeling of existing nigral neurons [13]. These data are in line with earlier studies showing that adult substantia nigra progenitor cells give rise to glial cells only [16]. However, the in vivo differentiation pattern may not reflect the entire lineage potential of resident progenitor cells, because regional environmental factors appear to restrict in situ differentiation to distinct neural lineages. For example, in vitro analysis and transplantation studies have suggested that progenitor cells from the adult substantia nigra, similar to progenitors from the adult spinal cord, have the potential to give rise to cells of all neural lineages [16–18]. In addition, isolated cortical progenitor cells have the potential to give rise to glia and neurons in vitro [19].

Clonogenic neural stem cells (NSCs) are self-renewing cells that maintain the capacity to differentiate into brain-specific cell types and may also replace or repair diseased brain tissue. Multipotent NSCs with the potential to generate mature cells of all neural lineages, including astroglia, oligodendroglia, and neurons, have been consistently demonstrated within the hippocampus and the SVZ of lateral ventricles [20–26]. These cells grow in vitro as spherical floating clusters (neurospheres) in the presence of epidermal growth factor (EGF) [21, 27]. Previous work has reported that SVZ NSCs correspond to a rare population of relatively quiescent cells. More recently, it has been suggested that not the ciliated ependymal cells correspond to the NSCs [24] but that SVZ astrocytes act as NSCs in both the normal and regenerating adult brain [28]. Recent studies demonstrated the presence of multipotent central nervous system (CNS) stem cells in non-neurogenic regions of the adult brain, including the spinal cord and the ventricular neuraxis [17, 18]. In contrast to SVZ NSCs, the proliferation of these NSCs depends on both EGF and fibroblast growth factor-2 (FGF-2) [18, 26]. Lie and coworkers described the isolation of multipotent NSCs from the adult substantia nigra with neurogenic differentiation capacity in vitro and after transplantation into the adult hippocampus [16]. However, the authors neither reported on detailed characterization of these progenitor cells in vitro nor provided data on neuronal subtype specification or functional properties after differentiation. Moreover, similar to all other adult CNS stem cells, these midbrain-derived NSCs did not differentiate into dopaminergic nerve cells [16].

Here, we show the presence of multipotent clonogenic NSCs in the adult mouse tegmentum (tegmental NSCs [tNSCs]) with all major properties of CNS stem cells such as neurosphere formation, expression of Nestin and other NSC markers, as well as significant telomerase activity. They show the capacity to differentiate in vitro into all neural cell lineages, including astroglia, oligodendroglia, and neurons. Moreover, the resulting nerve cells displayed morphological and functional properties of mature neuronal subpopulations, such as GABAergic and dopaminergic neurons.

Materials and Methods

Sphere Culture

Adult mice (6–10-week-old male C57BL/6 mice) were killed by cervical dislocation, and their brains were removed and placed into ice-cold Hanks' balanced saline solution supplemented with 1% penicillin/streptomycin and 1% glucose (all from Gibco, Tulsa, OK, http://www.invitrogen.com). The tegmental tissue (midbrain and hindbrain), including the subependymal zone/SVZ of the aqueduct and fourth ventricle, was then aseptically prepared using a dissection microscope. The meninges were carefully removed from the tissue after preparation of the tegmental area. For comparative studies with NSCs from adult's principal neurogenic regions, we isolated the hippocampus from the same mice as described previously [19]. For expansion of neurospheres, tissue samples from both regions were incubated in 0.1% trypsin (Sigma, St. Louis, http://www.sigmaaldrich.com) for 10 minutes at room temperature, incubated in DNase (40 mg/ml; Sigma) for 10 minutes at 37°C, and homogenized to a quasi–single-cell suspension by gentle triturating [29]. The cells were added to 25-cm^2 flasks (2–3 $\times$ 10^6 viable cells per flask) in serum-free Neurobasal (NBa) medium containing 1% glutamate, 2% B27 supplement, and 1% penicillin/streptomycin (all from Gibco) supplemented with 20 ng ml^{-1} of both mitogens FGF-2 and EGF (both from Sigma). After 10–20 days, sphere formation was observed. These neurospheres were expanded for an additional 3–12 weeks (in total, five to 10 passages) before terminal differentiation was initiated. The medium was changed once a week, and growth factors were added twice a week. For BrdU labeling, cells were incubated for 30 hours with 10 μM BrdU.

Differentiation Conditions

Induction of neural differentiation (protocol 1) was initiated by plating the cells on poly-L-lysine (PLL)-coated glass coverslips at a concentration of 1.5–2.0 $\times$ 10^5 cells cm^{-2} in NBa medium containing 1% glutamate, 2% B27 supplement, and 1% penicillin/streptomycin supplemented with 0.5 μmol l^{-1} all-trans-retinoic acid (Sigma), 10 ng ml^{-1} brain-derived neurotrophic factor (BDNF; Promega, Madison, WI, http://www.promega.com), and 100 μM dibuteryl(db)-cAMP (Sigma). Cells were differentiated for 14 days. For analyzing the differentiation capacity of tNSCs, several other combinations of growth factors/cytokines were used (Table 1). The following substances were used: 10% fetal bovine serum (Biochrom AG, Berlin, http://www.biochrom.de), 100 pg/ml interleukin (IL)-1b, 1 ng/ml IL-11, 10 ng/ml glial cell line–derived neurotrophic factor, 1 ng/ml leukemia inhibitory factor (all from Sigma), 10 ng/ml FGF-4, 10 ng/ml FGF-8, and 10 ng/ml sonic hedgehog (Shh; all from R&D Systems, Minneapolis, http://www.rndsystems.com). For co-culture analyses, various feeder cells (mouse embryonic fibroblasts [MEFs]), PA6 stromal cells, as well as cortical and striatal astrocytes from embryonic day 14.5 [E14.5] rat embryos) were cultured on gelatine-coated cover slides as described earlier [29, 30]. Before plating the tNSCs on the feeder layers, the cells were incubated with expansion media supplemented with 500 ng/ml Shh and 100 ng/ml FGF-8 for 48 hours ("pre-stimulation"). When co-culture was started, confluent feeder cells where washed twice with phosphate-buffered saline (PBS) and tNSCs were seeded at a concentration of

Table 1. Differentiation capacity of adult tegmental neural stem cells

Differentiation conditions (growth factors/cytokines/co-cultures)	MAP2ab$^+$ or Tuj1$^+$ neurons	GFAP$^+$ astrocytes	GalC$^+$ oligodendrocytes	TH$^+$ neurons
BDNF on PLL	+	+++	+	−
dbcAMP on PLL	+	+++	++	−
Retinoic acid on PLL	+	++++	−	−
BDNF, retinoic acid on PLL	+	++	+	−
BDNF, dbcAMP, retinoic acid on PLL (protocol 1)	+	++	+	−
FBS on PLL	+	+++	+	−
IL-1b on PLL	+	++	+	−
IL-1b, IL-11, GDNF, LIF on PLL	++	++++	++	−
FGF-4, Shh on PLL	+	++++	+	−
FGF-8, Shh on PLL	++	++++	+	−
dbcAMP, FGF-8, Shh on PLL	+	++	+	−
Pre-stimulation (FGF-8) on PLL	+	n.d.	n.d.	−
Pre-stimulation (FGF-8) + CM on PLL	++	n.d.	n.d.	−
Pre-stimulation (Shh) on PLL	++	n.d.	n.d.	−
Pre-stimulation (Shh) + CM on PLL	++	n.d.	n.d.	−
Pre-stimulation (FGF-8 + Shh) on PLL (protocol 2)	+	+++	n.d.	−
Pre-stimulation (FGF-8 + Shh) + CM on PLL	+	+++	n.d.	−
Pre-stimulation (FGF-8 + Shh) on MEFs (protocol 3)	++	+++	+	−
Pre-stimulation (FGF-8 + Shh) on cortical astrocytes	+	n.d.	n.d.	−
Pre-stimulation (FGF-8 + Shh) on striatal astrocytes	+	n.d.	n.d.	−
Pre-stimulation (FGF-8 + Shh) on PA6 cells (protocol 4)	++	+++	+	+

Immunostainings were scored as − if no cells were positive for the respective marker, + if up to 5% of cells were positive, ++ if 5%–25% of cells were positive, +++ if 25%–75% of cells were positive, and ++++ if more than 75% of cells were positive.
Abbreviations: BDNF, brain-derived neurotrophic factor; CM, conditioned medium on PA6 cells; dbcAMP, dibuteryl-cAMP; FBS, fetal bovine serum; FGF, fibroblast growth factor; GalC, galactocerebrosidase C; GDNF, glial cell line–derived neurotrophic factor; GFAP, glial fibrillary acidic proetin; IL, interleukin; LIF, leukemia inhibitory factor; MAP2ab, monoclonal antimicrotubule-associated protein 2ab; MEF, mouse embryonic fibroblast; n.d., not determined; PLL, poly-L-lysine; Shh, sonic hedgehog; TH, tyrosine hydroxylase.

1.5–2.0 $\times$ 10^5 cells cm^{-2} in Glasgow's modified Eagle's medium (Gibco) containing 1% glutamine, 1 mM sodium pyruvate, 0.1 mM nonessential amino acids, and 0.1 mM 2-mercaptoethanol ("differentiation medium" [DM]) supplemented with 10% knockout-serum replacement (Gibco). Medium change was performed on day 4 and every other day after that. After 7 days, the medium was changed to "differentiation medium" supplemented with 1% N2 (DM-N2 medium; Gibco).

Clonal Analysis

Clonal analysis was performed according to Uchida and coworkers [31]. In brief, tNSCs were serially diluted into expansion medium in 96-multiwell plates. On the next day, single cell–containing wells (assessed microscopically) were expanded by supplementing the medium to 50% with conditioned medium containing growth factors. Cells were expanded for 3–6 weeks and then differentiated using feeder cell–free differentiation protocol 1.

Flow Cytometry

tNSCs were treated with Accumax (Gibco) and washed with PBS. Dead cells were excluded from analysis by forward-scatter gating. Samples were processed using a FACSCalibur flow cytometer, and analyses were performed with the Cellquest software (both from Becton, Dickinson and Company, Franklin Lakes, NJ, http://www.bd.com). Antibodies were used as follows: CD34–fluorescein isothiocyanate (FITC) 1:10, CD45-phycoerythrin (PE) 1:10, CD24-FITC 1:200 (all from Chemicon, Temecula, CA, http://www.chemicon.com), rat anti-prominin1 monoclonal antibody 13A4 1:300 (BD Biosciences, San Diego, http://www.bdbiosciences.com), and mSSEA1 1:5 (kindly provided by Dr. Beltinger, University of Ulm) followed by fluorescence-labeled secondary antibodies (Jackson ImmunoResearch Laboratories, West Grove, PA, http://www.jacksonimmuno.com). Propidium iodide (PI)–fluorescence-activated cell sorting (FACS) was performed as previously described [32]. In brief, the cells were dissociated by trypsin (Gibco) and washed with PBS. The cells were fixed with 80% ice-cold ethanol and incubated at −20°C for 30 minutes. The cells were washed with PBS and PI-stained (0.5 mg/ml PI in 0.038 M sodium citrate buffer [pH 7.0]) for 30 minutes in the dark (37°C). Dead cells were excluded from analysis by forward-scatter gating. A minimum of 10,000–12,000 events were acquired for each sample.

Immunocytochemistry

Cell cultures were fixed in 4% paraformaldehyde in PBS or with 4% paraformaldehyde/PBS followed by ice-cold acidic ethanol and HCl for BrdU staining. Immunocytochemistry was carried out using standard protocols. Cell nuclei were counterstained with 4,6-diamidino-2-phenylindole (DAPI). The following primary antibodies were used: mouse anti-Tuj1 1:500 or rabbit anti-Tuj1 1:2,000 (Covance, Richmond, CA, http://www.covance.com), sheep or rabbit anti–tyrosine hydroxylase (TH) 1:200 (Pel-Freez, Rogers, AR, http://www.pel-freez.com), rabbit anti-serotonin (5-HT) 1:2,500 (DiaSorin, Stillwater, MN, http://www.diasorin.com), rabbit anti-cholineacetyltransferase 1:500, mouse anti-galactocerebrosidase C (GalC) 1:750, rabbit anti–glial fibrillary acidic protein (GFAP) polyclonal 1:1,000, mouse anti-Nestin monoclonal 1:500, anti-CD-24-FITC 1:200, rabbit anti-neurogenin2 1:500, rabbit anti-neuroD1 1:500, rabbit anti-Musashi1 1:500 (all from Chemicon), rabbit anti-Ki-67 1:500 (Novocastra Ltd., Newcastle upon Tyne, U.K., http://www.novocastra.co.uk), rabbit anti–γ-aminobutyric acid (GABA) 1:1,000, rabbit anti-glutamate 1:10,000 (both from Sigma), mouse anti-GFAP monoclonal 1:1,000, mouse anti–monoclonal antimicrotubule-associated protein 2ab (MAP2ab) 1:300 (all from BD Pharmingen, San Diego, http://www.bdbiosciences.com/pharmingen), rat anti–prominin1-FITC monoclonal antibody 13A4 1:800 (BD Biosciences), rat anti–PSA-NCAM (polysialylated neural cell adhesion molecule) 1:250 (BD Pharmingen), rabbit anti-olig2 1:1,000 (kindly provided by Dr. Takebayashi; [33]) and fluorescence-labeled secondary antibodies (Jackson ImmunoResearch Laboratories), and rat anti-BrdU 1:40 with fluorescence-labeled secondary antibody (both from Abcam, Cambridge, U.K., http://www.abcam.com). Images were captured using a fluorescence microscope (Axiovert 135; Zeiss, Oberkochen, Germany, http://www.zeiss.com) or a Leica TCS/NT confocal microscope (Leica, Heerbrugg, Switzerland, http://www.leica.com) equipped with krypton, krypton/argon, and helium lasers.

RNA Extraction and Quantitative Real-Time RT-PCR Analysis

Total cellular RNA was extracted from tNSCs and 14-day differentiated tNSCs (differentiation protocol 1) using RNAeasy total RNA purification kit followed by treatment with RNase-free DNase (Qiagen, Hilden, Germany, http://www.qiagen.com). Quantitative real-time one-step reverse transcription–polymerase chain reaction (RT-PCR) was carried out using the LightCycler System (Roche, Mannheim, Germany, http://www.roche.com), and amplification was monitored and analyzed by measuring the binding of the fluorescence dye SYBR Green I to double-stranded DNA. One microliter (50 ng) of total RNA was reverse-transcribed and subsequently amplified using QuantiTect SYBR Green RT-PCR Master mix (Qiagen) and 0.5 μmol l^{-1} of both sense and antisense primers. Tenfold dilutions of total RNA were used as external standards. Standards and samples were simultaneously amplified. After amplification, melting curves of the RT-PCR products were acquired to demonstrate product specificity. The results are expressed relative to the housekeeping gene *HMBS* (hydroxymethylbilane synthase). Primer sequences, lengths of the amplified products, and melting point analyses are summarized in Table 2.

Telomerase Activity

A highly sensitive in vitro assay known as the quantitative real-time telomeric repeat amplification protocol [34, 35] has been used for detecting telomerase activity (OTD kit; Allied Biotech, Inc., Ijamsville, MD, http://www.alliedbiotechinc.com). The telomerase activity in the cell or tissue extract is determined through its ability to synthesize telomeric repeats onto an oligonucleotide substrate in vitro. Telomerase from cell or tissue extracts adds telomeric repeats onto a substrate oligonucleotide, and the resulting extended products are subsequently amplified by the PCR. The PCR products are then visualized using the DNA fluorochrome SYBR Green as described above. Mouse embryonic stem cells (ESCs) (D3 ESC line) were used as positive control and cultured as described previously [36], whereas adult mouse cortical tissue was used as negative control [37].

Electrophysiology

Cells were investigated 7–20 days after differentiation using standard whole-cell patch-clamp technique. Data were recorded using an EPC-7 or EPC-9 amplifier (HEKA Electronics Inc., Lambrecht/Pfalz, Germany, http://www.heka.com) and pClamp data acquisition software (Axon Instruments, Union City, CA, http://www.moleculardevices.com) essentially as described previously [38, 39]. Extracellular solution contained (in mmol l^{-1}) 142 NaCl, 8.1 KCl, 1 $CaCl_2$, 6 $MgCl_2$, 10 HEPES, and 10 D-glucose (pH 7.4; 320 mOsm). Pipette solution contained (in mmol l^{-1}) 153 KCl, 1 $MgCl_2$, 5 EGTA, and 10 HEPES (pH 7.3; 305 mOsm). Using these solutions, borosilicate pipettes had resistances of 6–10 MΩ. Seal resistances in the whole-cell mode were between 0.1 and 1 GΩ. For recordings of GABA-induced inward currents, the solutions were balanced giving an equilibrium potential of 0 mV for chloride ions. For recordings of glutamate-induced inward currents, the external bath solution contained (in $mmol^{-1}$) 162 NaCl, 1.2 $CaCl_2$, 2.4 KCl, 0.01 glycine, 11 glucose, 10 HEPES (pH 7.3; 320 mOsm). Picrotoxin (100 μM; Sigma) and strychnine (2 μM; Sigma) were added to inhibit ligand-gated chloride channels. The internal solution contained (in $mmol^{-1}$) 95 CsCl, 6 $MgCl_2$, 1 $CaCl_2$, 10 HEPES, and 11 EGTA (pH 7.2; 300 mOsm). Drugs were applied rapidly via gravity with an SF-77B perfusion fast-step system (Warner Instruments LLC, Hamden, CT, http://www.warnerinstruments.com). Data were analyzed using pClamp 8.0, Microsoft Excel 97 (Microsoft, Redmond, WA, http://www.microsoft.com), and Origin 5.0 software. Resting membrane potentials (RMP) were determined immediately after gaining whole-cell access. Action potentials (APs) were elicited by applying increasing depolarizing current pulses (10-pA current steps). The afterhyperpolarization (AHP) amplitude was measured from peak to beginning of plateau reached during the current injection, AP duration was measured at half amplitude, and time to peak AHP from spike onset.

Determination of Dopamine, GABA, and Serotonin Production and Release

For determination of dopamine production and release, media were supplemented with 100 μmol l^{-1} tetrahydrobiopterin and 200 μmol l^{-1} ascorbate 2 days prior to medium harvest. Dopamine levels were determined in medium, and extracellular buffer was stabilized with EGTA/glutathione solution as reported previously [29] and stored at −80°C until analysis.

Table 2. Primers for quantitative real-time reverse transcription–polymerase chain reaction

Gene (protein)	Sequence (forward; reverse)	Product length (bp)	Melting point analysis[a]
DDC (Dopa-decarboxylase)	5′-GTG GGT GAA GAG GAC TGA-3′ 5′-GCA GCC CCT TGA CTC CGT A-3′	182	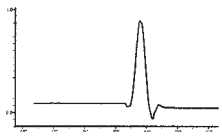
DAT (Dopamine transporter)	5′-ATG CTG CTC ACT CTG GGT ATC-3′ 5′-CAG GAA AGT AGC CAG GAC AAT-3′	135	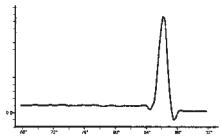
GFAP (Glial fibrillary acidic protein)	5′-GAT CTA TGA GGA GGA AGT TCG-3′ 5′-TCT GCA AAC TTA GAC CGA TAC C-3′	183	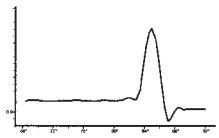
HMBS (Hydroxymethylbilane synthase)	5′-TGT ATG CTG TGG GTC AGG GAG-3′ 5′-CTC CTT CCA GGT GCC TCA GA-3′	144	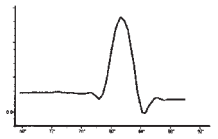
MBP (Myelin basic protein)	5′-CAC GGG CAT CCT TGA CTC-3′ 5′-GCC GTG CTG CGA CTT C-3′	130	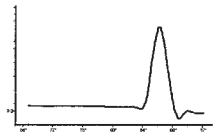
MSI1 (Musashi 1)	5′-GCA GAC CAC GCA GGA AG-3′ 5′-CGC CAG CAC TTT ATC CAC-3′	151	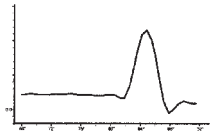
NeuroD1 (Neurogenic differentiation 1)	5′-CCG CCA CAC GCC TAC A-3′ 5′-CAA ACT CGG CGG ATG G-3′	148	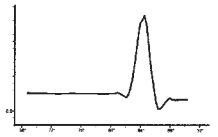
Neurog2 (Neurogenin 2)	5′-CGG CGT CAT CCT CCA AC-3′ 5′-CGG GTA GAG GAC GAG AGA GG-3′	179	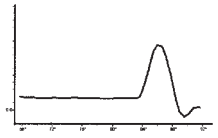
NES (Nestin)	5′-TGG AAC AGA GAT TGG AAG GC-3′ 5′-TCT TGA AGG TGT GCC AGT TGC-3′	153	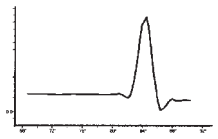
NF (Neurofilament-160kd)	5′-CAT CAG CAA GTC GGT AAA GG-3′ 5′-CTG CGG GCT ACG GTC A-3′	133	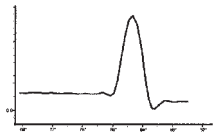

Continued on following page

Table 2. (Continued)

Gene (protein)	Sequence (forward; reverse)	Product length (bp)	Melting point analysis[a]
NTRK1 (Neurotrophic tyrosine kinase, receptor, type 1)	5′-GAG TTG AGA AGC CTA ACC ATC-3′ 5′-GCA TTG GAG GAC AGA TTC AGG-3′	104	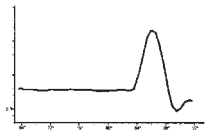
NR4A2 (Nuclear receptor Nurr1)	5′-TGT CAG CAC TAC GGT GTT CG-3′ 5′-AGG GTA AAC GAC CTC TCC G-3′	2,263	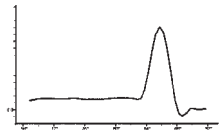
Olig2 (Oligodendrocyte transcription factor 2; Olig2)	5′-GAC CGA GCC AAC ACC AGC-3′ 5′-GGG ACG ATG GGC GAC TAG-3′	166	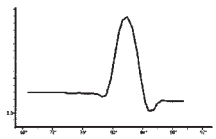
Pax6 (Paired box protein PAX6)	5′-GCA CCA AAG GGT CAT CGC-3′ 5′-TGG GGG GTG GAT GGA AG-3′	193	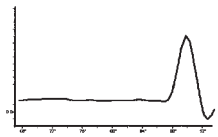
PLP (Myelin proteolipid protein)	5′-CAC CTA TGC CCT GAC TGT TG-3′ 5′-GTG GAA GGT CAT TTG GAA CAT A-3′	176	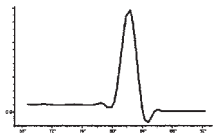
TH (Tyrosine hydroxylase)	5′-AGC TCC TGC ACT CCC TGT C-3′ 5′-CGA GAG GCA TAG TTC CTG AGC-3′	175	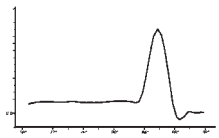

[a]The *x*-axis represents temperature (from 68°C–92°C in 4°C steps), and the *y*-axis indicates fluorescence -d(F1)dT.

Dopamine was assayed by reverse-phase high-performance liquid chromatography (HPLC) with an electrochemical detector as previously described [40]. GABA and serotonin were assayed by HPLC with fluorescence detection [40], employing precolumn derivatisation with ortho-phthaldialdehyde and an automatic HPLC system (Kontron Instruments, Neufahrn, Germany). The excitation and emission wave lengths of the fluorescence detector were set at 330 and 450 nm, respectively.

Cell Counting and Statistics

For quantification of the percentage of cells producing a given marker, in any given experiment the number of positive cells of the whole well surface was determined relative to the total number of DAPI-labeled nuclei. In a typical experiment, a total of 500–1,000 cells were counted per marker. Statistical comparisons were made by Dunnett's *t* test. If data were not normally distributed, a non-parametric test (Mann-Whitney *U* test) was used for comparisons of results. All data are expressed as mean ± SEM.

RESULTS

Isolation and In Vitro Characterization of Neurosphere-Forming Cells from the Adult Tegmentum

To isolate tNSCs, the tegmentum (midbrain and hindbrain) was selectively dissected from adult C57BL/6 mice using a dissection microscope. Cells were isolated and cultured in uncoated flasks in serum-free NBa medium supplemented with EGF and FGF-2. After 10–20 days in vitro, the cells formed small spheres with all typical morphological properties of neurospheres (Fig. 1A). FACS analysis revealed that the phenotype of the tNSCs was $CD24^{low/-}$, $CD34^-$, $CD45^-$, $Prominin1^-$, and $SSEA1^-$ (Fig. 1B). Furthermore, we used quantitative real-time RT-PCR and immunocytochemistry on unfixed or fixed neurospheres to investigate the expression pattern of several early and late neuroectodermal genes (Fig. 2A, 2C; for complete names of genes and encoded proteins, refer to Table 2). tNSCs expressed high levels of early neuroectodermal markers such as Nestin, an

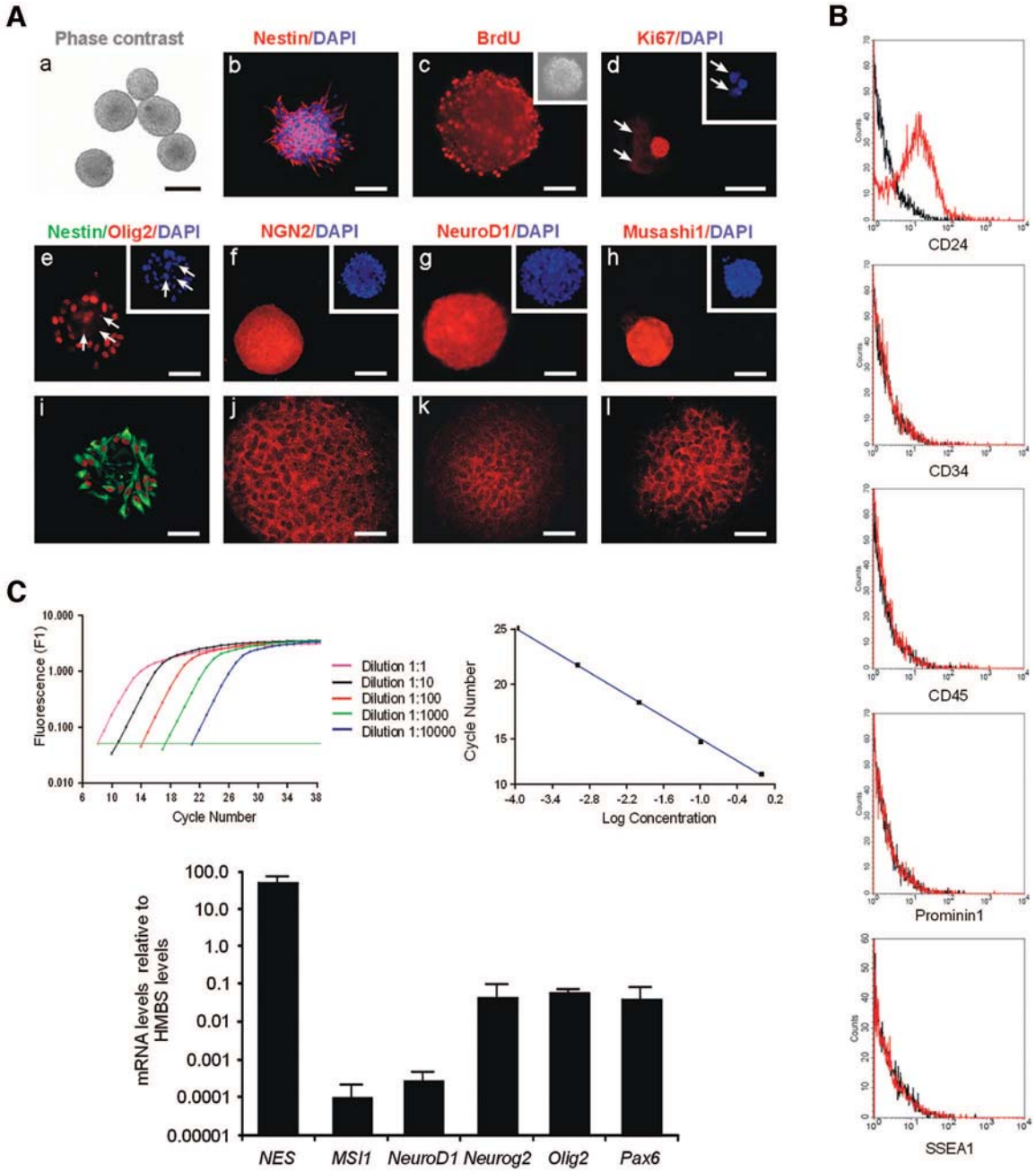

Figure 1. Characteristics of adult tNSCs during in vitro expansion. **(A):** Morphology and marker expression of adult tNSCs during expansion in the presence of EGF and FGF-2. Spheres were cultured for 2–3 hours to allow attachment and then stained for Nestin (b, i), Ki67 (d), Olig2 (e, i), Neurogenin2 (f, j), NeuroD1 (g, k), and/or Musashi1 (h, l). For BrdU staining (c), the spheres were cultured in the presence of 10 μM BrdU for 30 hours before plating. Nuclei were counterstained with DAPI. Confocal images (i–l) confirm the presence of the respective marker protein in nearly all cells within the neurosphere. Arrows mark Ki67$^-$/DAPI$^+$ cells (d) and apoptotic cells not expressing Nestin/Olig2 (e), respectively. Scale bars = 15 μm (d), 30 μm (e, i, j–l), 50 μm (b, c, f–h), and 200 μm (a). **(B):** Flow cytometry of tNSCs cultured for 4–12 weeks (five to 10 passages). Cells were labeled with fluorescence-coupled antibodies against CD24, CD34, CD45, prominin1, and SSEA1 or immunoglobulin isotype control antibodies. Cells were analyzed using a FACSCalibur flow cytometer. Black line, control immunoglobulin; red line, specific antibody. **(C):** Quantitative transcription profile of tNSCs. Top panel: Representative real-time RT-PCR analysis using the LightCycler technique. Plot of the fluorescence versus the cycle number obtained from SYBR Green detection of serially diluted *NES* mRNA (encoding for nestin). The crossing line represents the position of the threshold. Diagram on right shows the standard curve obtained by plotting cycle number of crossing points versus dilution factor. Bottom panel: Quantitative real-time RT-PCR analyses of NSC markers (*NES, MSI1*), proneural genes (*NeuroD1, Neurog2, Olig2*), and the neuronal transcription factor *Pax6* in tNSCs during expansion. Expression levels are expressed relative to the housekeeping gene *HMBS*. Data shown are mean values ± SEM from at least three independent experiments. For primers, complete names of genes, and melting curve analyses demonstrating the specificity of amplified PCR products, see Table 2. Abbreviations: BrdU, 5-bromo-2-deoxyuridine; DAPI, 4,6-diamidino-2-phenylindole; EGF, epidermal growth factor; FGF, fibroblast growth factor; HMBS, hydroxymethylbilane synthase; PCR, polymerase chain reaction; RT-PCR, reverse transcription–polymerase chain reaction; tNSC, tegmental neural stem cell.

intermediate filament protein present in CNS stem cells (Fig. 1A, 1C) [21, 41], and the CNS stem cell marker Musashi1 [42], as well as the proneural genes *Olig2*, *Neurogenin2*, and *NeuroD1* on both the mRNA and protein levels (Fig. 1A, 1C). Proneural genes, which encode transcription factors of the basic helix-loop-helix class, are important factors for NSC self-renewal, multipotency, and commitment to neural lineages of NSCs [43–48]. Confocal microscopy of the spheres revealed that nearly all (>95%) living cells without nuclear condensation (DAPI stain) expressed Nestin (Fig. 1A) with some cells (<5%) being double-positive for Nestin and GFAP (data not shown). Co-labeling with anti-olig2 antibody further demonstrated co-expression of both early neuroectodermal markers in nearly all living cells (Fig. 1A). Furthermore, the proneural genes *Neurogenin2* and *NeuroD1*, as well as the NSC marker *Musashi1*, were expressed in nearly all cells within the neurospheres as shown by confocal microscopy (Fig. 1A). The neurogenic fate-determining transcription factor Pax6 mRNA was also expressed in these neurospheres (Fig. 1C). Only very few cells were weakly positive for CD24 or PSA-NCAM protein (data not shown). Markers for mature neural cell types, such as *MBP*, *PLP*, *NTRK1, MAP2*, and *TH*, were undetectable or very low at the mRNA level; at the protein level, MAP2ab, GalC, and TH were absent (data not shown). This phenotype is similar to that of NSCs derived from adult mouse SVZ or hippocampus [20, 22, 23]. tNSCs could be passaged and cultured as secondary and tertiary neurospheres without changing morphology and phenotype for 3–12 weeks (~5–10 passages).

Cell Cycle Distribution, Proliferation Potential, and Apoptosis of tNSCs

Cell cycle analysis using PI-FACS demonstrated that, besides apoptosis (see below), there was a large fraction of tNSCs distributed in G_1, S, and G_2/M phases (see Fig. 2A, 2B for details of cell cycle distribution). In addition, we used the proliferation marker Ki67 as well as BrdU incorporation to identify DNA-synthesizing cells (Figs. 1A and 2B). Ki67 was detected in the nucleus of proliferating cells in all active phases of the cell cycle from the late G_1-phase through the M-phase but is absent in non-proliferating and early G_1-phase cells and in cells undergoing DNA repair [49–51]. As expected, total Ki67 staining (representing late G_1 through M phase) was higher than total BrdU staining at each time point. When the percentage of G_1-phase cells was subtracted from total Ki67 staining, the resulting percentage was very similar to that of BrdU-stained cells (Fig. 2B).

To evaluate cell death by apoptosis during cultivation of tNSCs, we used PI-FACS analysis and DAPI staining. After 4–12 weeks, an average number of 4% ± 1% of cells were found by PI-FACS analyses to be apoptotic. Histograms representing FACS analysis and DAPI staining of apoptotic events in tNSCs are shown in Figure 2B. Spontaneously apoptotic cells exhibited chromatin condensation and margination, sometimes followed by appearance of apoptotic bodies, as revealed by DAPI staining, and were negative for Ki67 (data not shown) as well as for most other markers tested such as Nestin and Olig2 (Fig. 1A).

Telomerase is inactive in most somatic cells but present in various stem cell populations [52–54]. Quantification of telomerase activity in tNSCs using the telomeric repeat amplification protocol [34, 35] showed stable telomerase activity in tNSCs over the 3-month expansion period with significantly higher activity compared to that measured in mouse cortical tissue (negative control) but lower activity compared to that in mouse ESCs (Fig. 2C). Together, investigations of the proliferation characteristics revealed the typical pattern of slowly dividing cells with a small amount of spontaneous apoptosis within the tNSC neurospheres, similar to fetal mouse mesencephalic NSCs [55].

Differentiation Capacity of Adult tNSCs

Differentiation of tNSCs was initiated after 3–12 weeks by removal of mitogens, plating the cells onto poly-L-lysine, and addition of BDNF, db-cAMP, and retinoic acid (protocol 1, Fig. 1A). After 14 days, the majority of cells (71% ± 27%) acquired morphologic and phenotypic characteristics of astrocytes ($GFAP^+$), 6% ± 5% acquired those of oligodendrocytes ($GalC^+$), and 5% ± 2% those of mature neurons ($MAP2ab^+$; $n = 8$; Fig. 3B). GFAP, GalC, and Tuj1/MAP2ab were never found in the same cell (Figs. 1D and 4A). Consistently, quantitative RT-PCR of tNSCs after differentiation using protocol 1 for 14 days confirmed the differentiation of tNSCs into mature neuroectodermal cells (Fig. 3E). The NSC marker gene *NES*

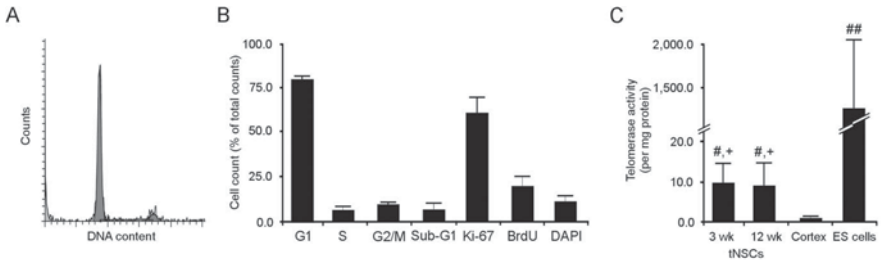

Figure 2. Cell cycle distribution, proliferation potential, and apoptosis of adult tNSCs. **(A):** PI-FACS analysis of tNSCs showing the cell cycle distribution typical for slowly dividing cells. **(B):** Quantitative data of PI-FACS analyses, Ki67 immunostaining, BrdU staining, and nuclei with chromatin clumping and fragmentations (apoptotic nuclei) in DAPI stainings. (See Fig. 2A for Ki67, BrdU, and DAPI stainings of neurospheres.) Results are the mean ± SEM from three to six independent experiments. **(C):** Telomerase activity in tNSCs after 3 and 12 weeks, respectively, as well as adult cortical tissue and mouse ESCs during expansion measured by the quantitative real-time telomeric repeat amplification protocol. Telomerase activity was normalized to protein content. Results are mean values ± SEM from three independent experiments. #$p < .05$, ##$p < .001$ when compared with adult cortical tissue; +$p < .001$ when compared with ESCs. Abbreviations: BrdU, 5-bromo-2-deoxyuridine; DAPI, 4,6-diamidino-2-phenylindole; ESC, embryonic stem cell; PI-FACS, propidium iodide–fluorescence-activated cell sorting; tNSC, tegmental neural stem cell.

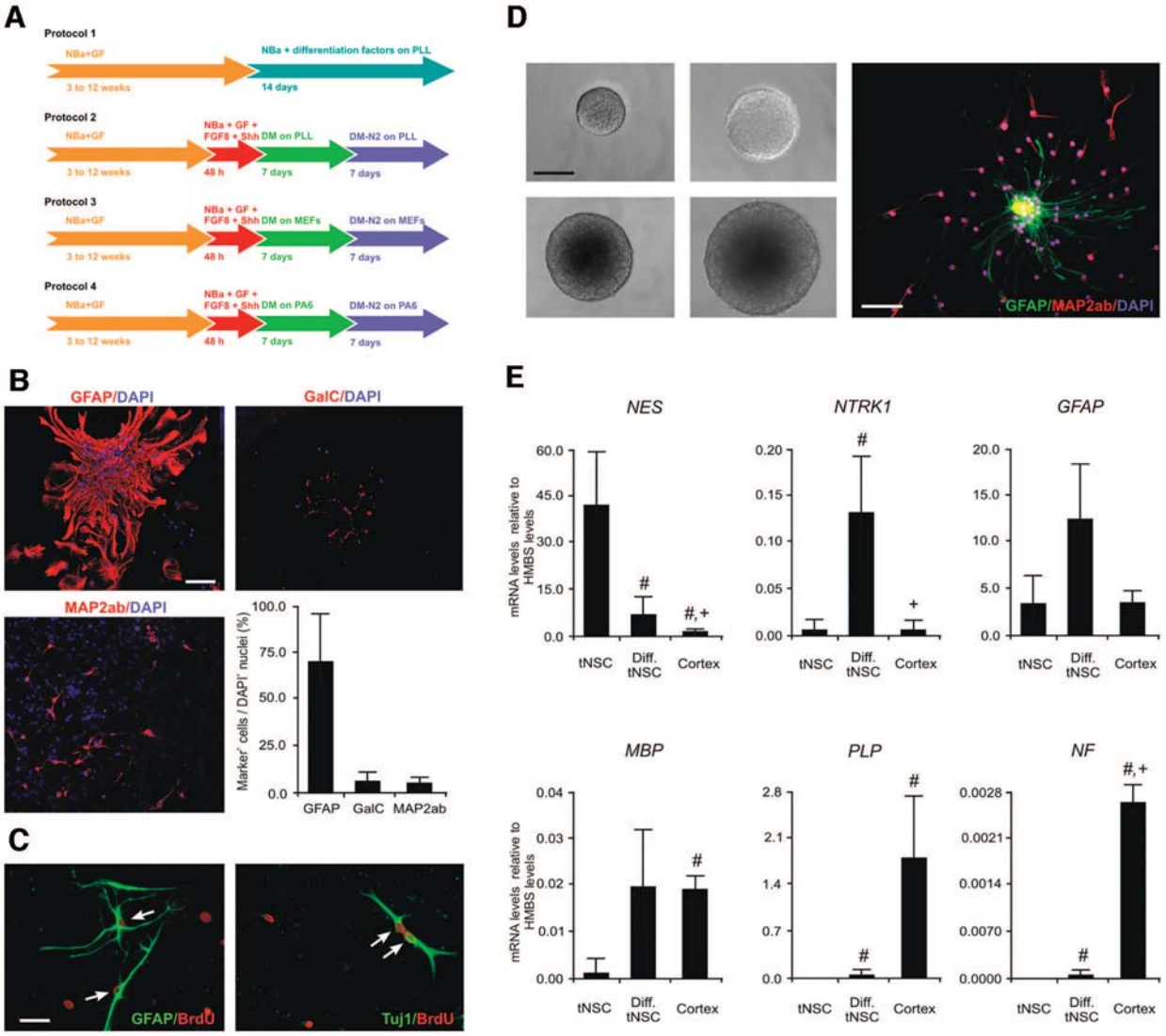

Figure 3. In vitro differentiation capacity of tNSCs. **(A):** Schematic diagrams of protocols for differentiation of tNSCs (see Materials and Methods for details). **(B):** tNSCs differentiated using protocol 1 were stained against markers for astrocytes (GFAP), oligodendrocytes (GalC), or neurons (MAP2ab). Nuclei are counterstained with DAPI (blue). Scale bar = 30 μm. Quantification of differentiation capacity of 14-day cultures of tNSCs differentiated using protocol 1. Data shown are mean values ± SEM from eight independent experiments. **(C):** Immunocytochemical analysis of differentiated tNSCs expanded for only 7 days. Prior to differentiation, tNSCs were incubated with 10 μM BrdU for 30 hours and then differentiated using protocol 1 and double-stained against GFAP or Tuj1 (green) and BrdU (red). Arrows indicate double-labeled cells. Scale bar = 15 μm. **(D):** Clonal analysis of single tNSCs. Left panel: Secondary neurospheres can be derived from a single tNSC from expanded neurospheres. Scale bar = 200 μm. Right panel: Differentiation capacity of clonally derived neurosphere cells. Progeny of single cell–derived neurospheres can be differentiated into neurons (MAP2ab) and astrocytes (GFAP). Nuclei were counterstained with DAPI (blue). Scale bar = 30 μm. **(E):** Quantitative transcription profile of tNSCs, differentiated tNSCs using protocol 1, and primary mouse cortical tissue. Results of quantitative real-time RT-PCR analyses of the NSC marker gene Nestin (*NES*), the neural gene *NTRK1,* glial genes (*GFAP, MBP, PLP*), and the neuronal gene *NF* are displayed. Expression levels are expressed relative to the housekeeping gene *HMBS*. For primers, complete names of genes, and melting curve analyses demonstrating the specificity of amplified PCR products as listed in Table 2. Results are mean values ± SEM from at least three independent experiments. $^{\#}p < .05$ when compared with tNSCs; $^{+}p < .05$ when compared with differentiated tNSCs. Abbreviations: BrdU, 5-bromo-2-deoxyuridine; DAPI, 4,6-diamidino-2-phenylindole; DM, differentiation medium; DM-N2, differentiation medium supplemented with N2; FGF, fibroblast growth factor; GalC, galactocerebrosidase C; GF, growth factor; GFAP, glial fibrillary acidic protein; MAP2ab, microtubule-associated protein 2ab; MEF, mouse embryonic fibroblast; NBa, neurobasal medium; NF, neurofilament; NSC, neural stem cell; PLL, poly-L-lysin; RT-PCR, reverse transcription–polymerase chain reaction; Shh, sonic hedgehog; tNSC, tegmental neural stem cell.

(encoding Nestin) was downregulated sixfold, whereas mRNA levels of *NTRK1*, *GFAP*, *MBP*, *PLP*, and *NF* increased six- to 430-fold during the differentiation process (Fig. 3E). Most mRNA levels of markers for mature neural cell types in differentiated tNSCs were lower compared with those in adult mouse cortex (Fig. 3E). No dopaminergic or serotoninergic cells could be detected using protocol 1. Replacement of BDNF/db-cAMP/retinoic acid by various combinations of growth factors/cytokines known to induce the dopaminergic phenotype in several murine stem cell types [38] led to changes in the differentiation

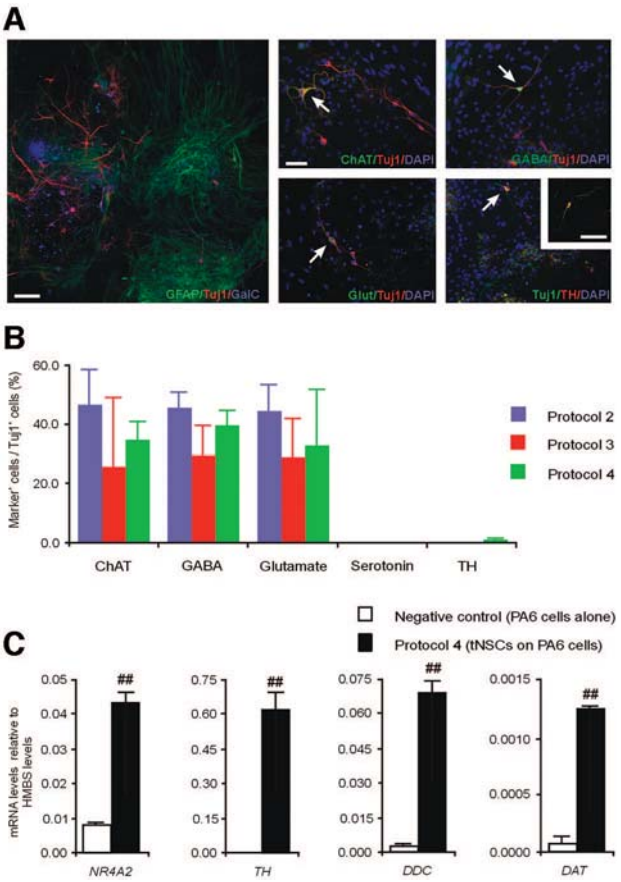

Figure 4. Neuronal subtype differentiation capacity of tNSCs in vitro established by using differentiation protocols 2–4 after an expansion phase of 3–12 weeks. **(A):** Triple immunostaining of tNSCs differentiated using protocol 4 for markers of astroglia (GFAP), neurons (Tuj1), and oligodendroglia (GalC), as well as cholinergic (ChAT), GABAergic (GABA), glutamatergic (glutamate), and dopaminergic (TH) neurons. Nuclei were counterstained with DAPI (blue). Arrows mark double-stained neurons. The inset shows high-magnification confocal image of a $Tuj1^+/TH^+$ neuron. Scale bars = 30 μm (left panel) or 15 μm. **(B):** Quantitative data of triple immunostainings of tNSCs differentiated with protocols 2–4, respectively. Results are mean values ± SEM from at least three independent experiments. **(C):** Quantitative real-time RT-PCR analyses of the dopaminergic marker genes nuclear receptor Nurr1 (*NR4A2*), TH (*TH*), dopa-decarboxylase (*DDC*), and dopamine transporter (*DAT*) on tNSCs differentiated using protocol 4 (closed bars) and negative control (open bars). Expression levels are expressed relative to the housekeeping gene *HMBS*. For primers, complete names of genes, and melting curve analyses, see Table 2. Results are mean values ± SEM from at least three independent experiments. $^{\#\#}p < .01$ when compared with negative control (PA6 cells alone). Abbreviations: ChAT, cholineacetyltransferase; DAPI, 4,6-diamidino-2-phenylindole; DAT, dopamine transporter; DDC, dopa-decarboxylase; GABA, γ-aminobutyric acid; GalC, galactocerebrosidase C; GFAP, glial fibrillary acidic protein; HMBS, hydroxymethylbilane synthase; RT-PCR, reverse transcription–polymerase chain reaction; TH, tyrosine hydroxylase; tNSC, tegmental neural stem cell.

capacity into astroglial, oligodendroglial, and neuronal cells, but no TH^+ neurons were observed (Table 1). For analyzing the differentiation capacity of acutely isolated tNSCs before neurosphere formation (7 days after preparation), we used the BrdU incorporation assay. The tNSCs were incubated during the expansion phase with BrdU (10 μM) for 30 hours. Then, differentiation was initiated using protocol 1. We were able to detect $BrdU^+/Tuj1^+$ neurons and $BrdU^+/GFAP^+$ glial cells (Fig. 3C), demonstrating that these neurons and glial cells were de novo–generated from proliferating progenitor cells.

Next, we tested various multistep protocols with pre-stimulation using FGF-8 and/or Shh for 48 hours in expansion medium before plating the cells on PLL or feeder layers of several cell types, including astroglia, MEFs, and PA6 stromal cells (protocols 2–4; Fig. 3A). In fact, protocol 4 is similar to the protocol for dopaminergic differentiation of mouse ESCs reported by Kawasaki and coworkers [30]. There were no relevant differences in the differentiation capacity of tNSCs into astroglia and neurons with respect to the various differentiation conditions (Table 1). In contrast, only protocol 4 was able to induce dopaminergic neurogenesis in a small percentage of cells (2.4% ± 1.4% of $Tuj1^+$ cells; $n = 3$), showing typical morphological features of $Tuj1^+/TH^+$ dopaminergic neurons with small irregularly shaped soma and bipolar or multipolar branching processes with varicosities (Fig. 4A, 4B). Using quantitative RT-PCR, we consistently demonstrated expression of various dopaminergic marker genes, including *NR4A2* (encoding the nuclear receptor Nurr1), *TH* (TH), *DDC* (dopa-decarboxylase), and *DAT* (dopamine transporter), in tNSCs differentiated using protocol 4 (Fig. 4C). No dopaminergic neurogenesis could be observed in cultures without PA6 cells (including protocols using PA6 conditioned media), and there were no differences in the amounts of glutamatergic, GABAergic, cholinergic, and serotoninergic neurons in cultures with PA6 cells compared with PA6 cell–free cultures (Fig. 4B; Table 1). Remarkably, the morphology of the different nerve cell subtypes was significantly different with large soma and multiple neurites in cholinergic cells and relatively small soma with two to three neurites in GABAergic and glutamatergic neurons as described for primary cultures (Fig. 4A). In contrast, protocol 4 also induced glutamatergic, GABAergic, and cholinergic neurons out of corresponding adult mouse hippocampal NSCs but was unable to produce TH^+ dopaminergic cells out of hippocampal NSCs (data not shown).

Clonal Analysis of Adult tNSCs

To determine whether individual tNSCs could generate both neurons and glia, neurospheres were dissociated and individual cells were isolated by the single-cell culture technique in ultra low–attachment multiwell-plates. Single cells were cultured in expansion medium for 3–6 weeks. One third of the single cells proliferated to generate secondary neurospheres (Fig. 3D). Clonal cells were then differentiated for 14 days using differentiation protocol 1. Double immunostaining revealed that each of these clonally derived neurospheres differentiated into neurons and astrocytes (Fig. 3D). In addition to the BrdU incorporation experiments (Fig. 3C), these results demonstrate that neurons and glia are de novo–generated from proliferating tNSCs.

Functional Properties of Differentiated Adult tNSCs

To analyze the functional properties of differentiated tNSCs, we performed whole-cell voltage-clamp recordings to measure voltage-gated sodium and potassium currents and current-clamp recordings to measure the capacity to generate action potentials

after differentiation for 10–20 days using protocol 1. The RMP of differentiated tNSCs was −46 ± 4 mV (n = 34), the input resistance was 536 ± 45 MΩ (n = 48), and the cell membrane capacity was 14.7 ± 1.3 pF (n = 48). Of differentiated tNSCs, 83 out of 95 recorded cells (87.4%) expressed a sustained outward current of a few hundred pA up to 5 nA (Fig. 5A). These currents showed a voltage dependence and kinetics characteristic for A-type currents as well as tetraethylammonium-sensitive delayed rectifier potassium channels (Fig. 5A, 5B). In 67 out of 95 cells (70.5%), we could identify inward currents of up to 2 nA with voltage dependence and kinetics typical for voltage-activated sodium channels (Fig. 5C, 5D). These currents were tetrodotoxin (TTX)-sensitive (Fig. 5C). Current-clamp recordings revealed that differentiated tNSCs generated TTX-sensitive APs with a duration of 9.6 ± 0.2 ms (n = 8) and a short AHP (Fig. 5E). The length of AHPs was 22.7 ± 0.8 ms, and the maximal amplitude 9.8 ± 0.4 mV (n = 8).

To further characterize the functional properties of differentiated tNSCs, we measured the response of tNSCs differentiated for 7 days using protocol 1 to various concentrations of GABA (10–1,000 μM), glutamate (1–300 μM), or *N*-methyl-D-aspartate (NMDA; 100 μM). GABA elicited inward currents in a dose-dependent manner with a half-maximal effective concentration (EC_{50} value) of 42 μM (Fig. 6A, 6B). These currents could be antagonized by co-application of bicuculline and enhanced by co-application of diazepam (Fig. 6C). The characteristics of GABA-induced currents in our cells are typical for $GABA_A$ receptors. Furthermore, glutamate induced fast inward currents in a dose-dependent manner with an EC_{50} value of 8 μM (Fig. 6D, 6E). Nine out of 10 cells expressing glutamate-induced currents also showed functional NMDA receptors with amplitudes of approximately 27% of the mean glutamate amplitude (Fig. 6F). Because there is no reliable evidence for functional glutamate receptors of the NMDA subtype in glial cells [56], these data further demonstrate functional properties of mature nerve cells.

Neurotransmitter (dopamine and GABA) production and release were studied on tNSCs differentiated using protocol 4.

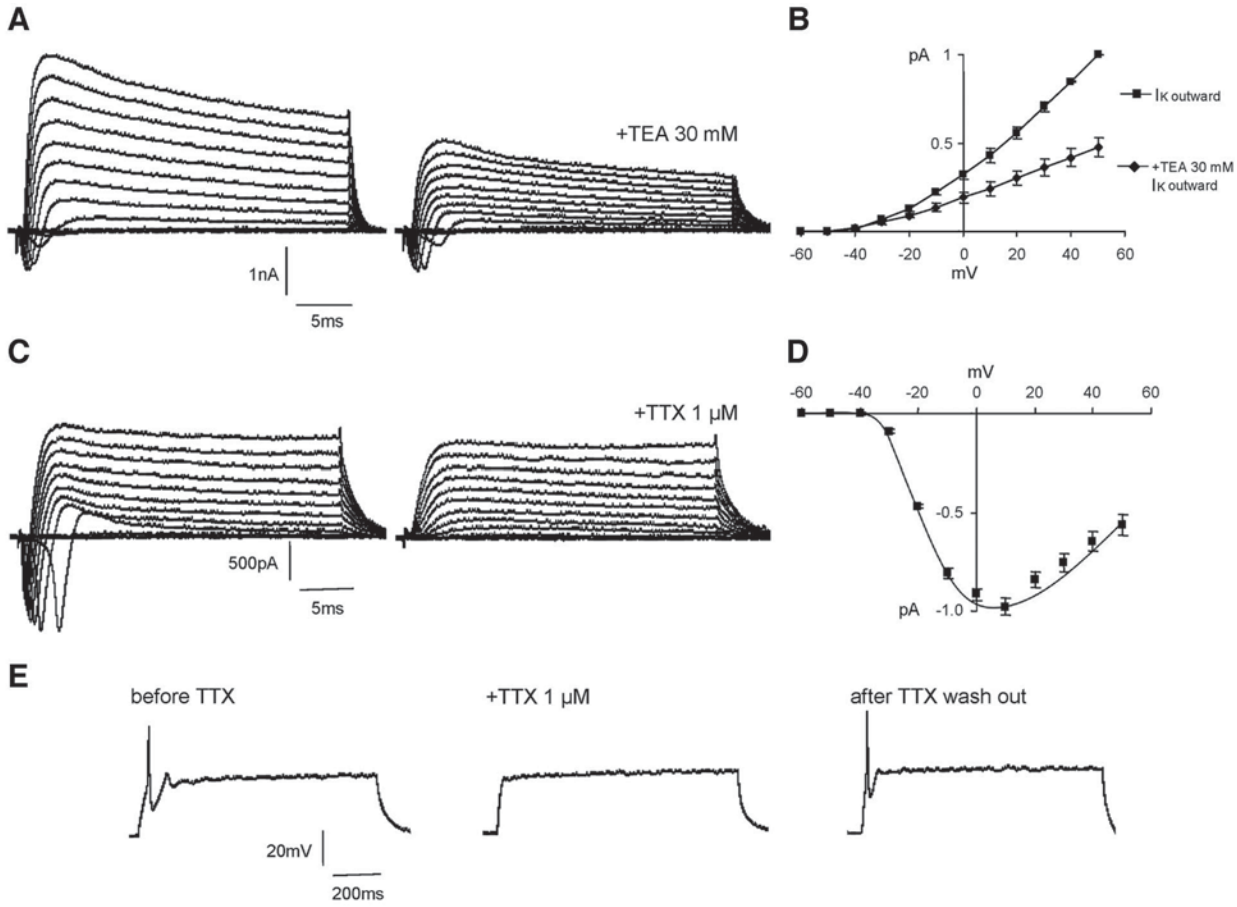

Figure 5. Electrophysiological properties of adult tegmental NSCs differentiated using protocol 1 for 10 days. For voltage-clamp measurements **(A–D)**, cells were held at −70 mV and depolarized to +50 mV with increasing amplitudes in steps of 10 mV. **(A):** Representative traces from a differentiated tNSC displaying inward and sustained outward currents. Potassium outward currents were markedly reduced by application of TEA (30 mM). **(B):** Current-voltage (I-V) relationships of the outward currents in steady state at the end of the voltage steps in the absence (■) and presence of 30 mM TEA (♦). Data are mean values ± SEM from three to 11 independent experiments. **(C–D):** Fast inward currents could be completely blocked by application of TTX (1 μM) and displayed the characteristic I-V relationship of voltage-gated sodium channels (n = 7). **(E):** Current-clamp recordings of the same cell recorded in **(C)** in response to depolarizing current pulses of increasing amplitude. The resting membrane potential was approximately −65 mV, and TTX-sensitive action potentials peaked at approximately +40 mV. Abbreviations: TEA, tetraethylammonium; tNSC, tegmental neural stem cell; TTX, tetrodotoxin.

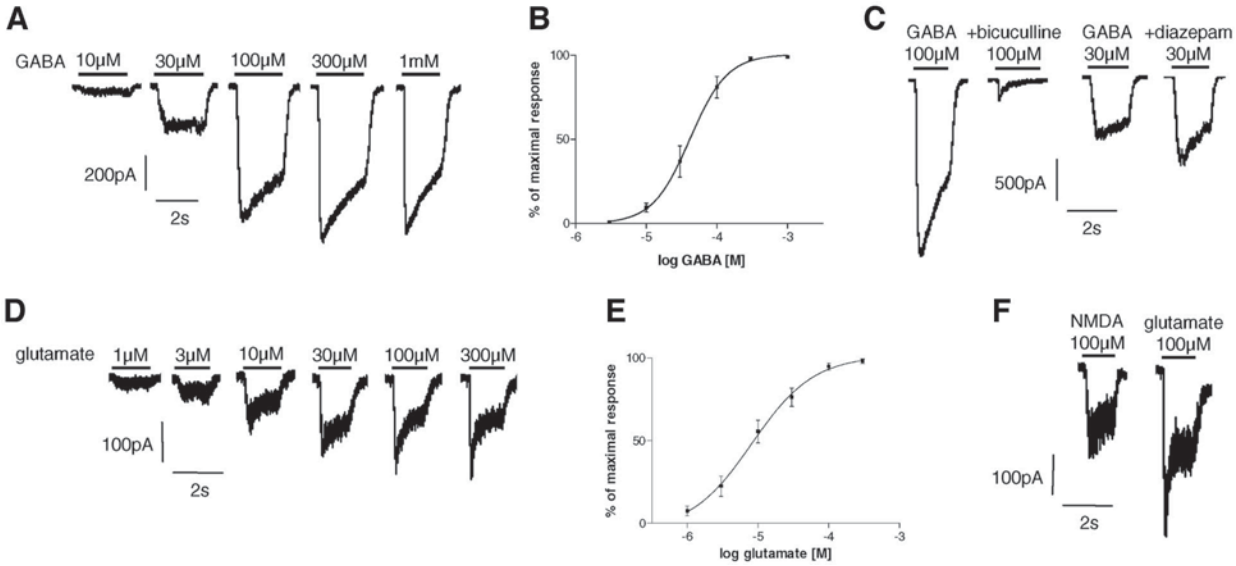

Figure 6. Electrophysiological properties of ligand-gated ion channels in adult tegmental neural stem cell (tNSCs) after in vitro differentiation for 7 days using differentiation protocol 1. The holding potential was −70 mV in whole-cell voltage-clamp mode, and substances were applied with a rapid perfusion system every 30 seconds. **(A):** Representative recordings of GABA-induced inward currents after applications of increasing concentrations of GABA (10–1,000 μM). **(B):** GABA dose-response curve with an half-maximal effective concentration (EC_{50}) value = 41.5 ± 1.1 μM. Data are mean values ± SEM from five independent experiments. **(C):** GABA-induced currents could be antagonized by co-application of bicuculline and enhanced by co-application of diazepam. **(D):** Representative recordings of glutamate-induced inward currents after applications of increasing concentrations of glutamate (1–300 μM). **(E):** Glutamate dose-response curve with an EC_{50} value = 8.2 ± 1.8 μM. Data are mean values ± SEM from eight independent experiments. **(F):** NMDA-induced currents could be elicited in nine out of 10 cells expressing glutamate-induced currents (mean NMDA amplitude was 27% of mean glutamate amplitude). Abbreviations: GABA, γ-aminobutyric acid; NMDA, *N*-methyl-D-aspartate.

HPLC electrochemical detector analysis showed significant amounts of dopamine in media conditioned by differentiated tNSCs for 2 days (38.3 ± 10.7 pg/ml; $n = 4$; Fig. 7A, 7B), but only small amounts of dopamine were found in extracellular buffer or after stimulation of the cells with 56 mM KCl for 45 minutes. (Fig. 7B), consistent with the amounts of TH^+ cells and the expression of various dopaminergic marker genes, including the key enzymes of dopamine synthesis (TH and dopa-decarboxylase; Fig. 4). Under the same conditions, we detected GABA production and potassium-dependent release of GABA by differentiated tNSCs (Fig. 7B). There was no dopamine production by undifferentiated tNSCs or tNSCs differentiated using protocol 1. Consistent with the immunocytochemical data, we did not find the neurotransmitter serotonin in any sample.

DISCUSSION

Here, we provide evidence for the existence of multipotent NSCs in the adult mouse tegmentum (midbrain and hindbrain region) with the capacity to differentiate in vitro into functional

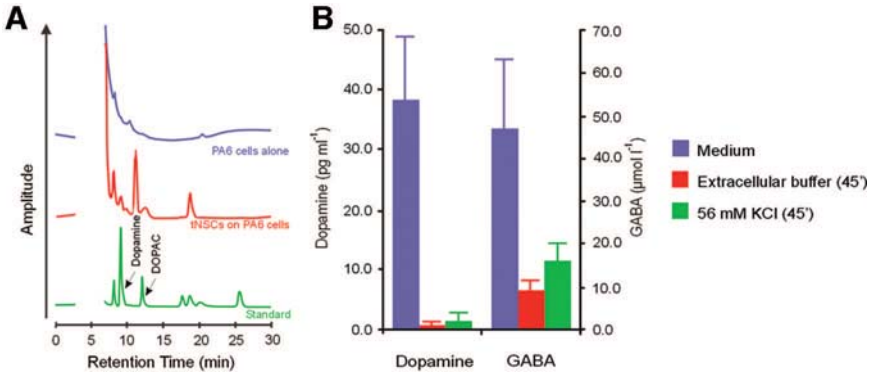

Figure 7. Neurotransmitter (dopamine, GABA) production and release of tNSCs differentiated on PA6 cells using protocol 4. **(A):** Representative chromatograms of HPLC-ECD determination of dopamine in medium conditioned for 2 days by tNSCs on PA6 cells (protocol 4, red) and PA6 cells alone (blue). Standard is presented in green. **(B):** Quantification of dopamine and GABA production in medium conditioned for 2 days (blue bars), in extracellular buffer conditioned for 45 minutes (red bars), and in extracellular buffer + 56 mM KCl conditioned for 45 minutes (green bars). Abbreviations: DOPAC, dihydroxyphenyl acetic acid; GABA, γ-aminobutyric acid; HPLC-ECD, high-performance liquid chromatography–electrochemical detector; KCl, potassium chloride; tNSC, tegmental neural stem cell.

nerve cell types, including dopaminergic neurons. We isolated and cultured NSCs from the adult tegmentum (tNSCs) of C57BL/6 mice using the neurosphere culture technique similar to those used for isolation and propagation of fetal mesencephalic NSCs [29, 38, 57, 58]. Their phenotype was similar to that of NSCs derived from adult mouse hippocampus, mouse SVZ, or human fetal brain samples [20, 31, 59]. The tNSCs were clonogenic, self-renewing cells that maintain the capacity to differentiate into mature functional nerve cells, including dopaminergic neurons (Figs. 3–7). Their potential to proliferate was slower compared with embryonic/fetal NSCs, whereas their differentiation capacity was similar to that of NSCs derived from fetal rodent or human mesencephalon [29, 38, 55, 57, 58, 60].

NSCs are often defined in vitro by the presence of the CNS stem cells marker Nestin [41, 61, 62], a class IV intermediate filament protein [61, 63, 64] and a marker for precursor cells in the adult brain [24, 61, 65–67]. Nestin is highly expressed in tNSCs during in vitro expansion. Furthermore, the RNA-binding protein Musashi1 is involved in post-transcriptional gene regulation in neuroprogenitors and/or NSCs and is used as a marker of those cell types [42]. Consistently, Musashi1 is expressed in tNSCs both at the mRNA and protein levels (Fig. 1). A large body of knowledge exists on lineage determination in NSCs, because unlike many types of stem cells, NSCs undergo self-renewal and multilineage differentiation in culture. Proneural genes, encoding transcription factors of the basic helix-loop-helix class, such as *NeuroD1*, *Neurogenin2*, and *Olig2*, are both necessary and sufficient to initiate the development of neural lineages and to promote the generation of progenitors that are committed to neural differentiation [43–45]. Proneural genes are therefore expressed mostly in neuroprogenitor cells, including NSCs in early neuroectodermal tissues [23, 46–48]. Consistently, tNSCs expressed mRNA and protein of NeuroD1, Neurogenin2, as well as Olig2 (Fig. 1). For example, *NeuroD1* and *Neurogenin2* are considered neuronal differentiation genes and promote exit from the cell cycle and inhibit gliogenesis [68–70]. In addition, Olig2 is a pivotal factor for neurogenesis and oligodendroglial specification of adult NSCs in vitro [23, 71]. Although Olig2 showed no co-localization with adult CNS stem cell markers in vivo, it becomes highly upregulated under expansion conditions with high levels of EGF and FGF-2 (Fig. 1 and [23]). Olig2 is required for the proliferation and self-renewal of neurosphere cells, as shown by interference analysis [23]. The transcription factor Pax6 is the major neurogenic determinant for radial glial cells and adult NSCs [23, 72–74]. Indeed, neurogenic differentiation in neurospheres fully depends on the expression of the transcription factor Pax6, independent of the region of origin [23]. Analysis of Pax6 expression in tNSCs demonstrated Pax6 expression during the expansion phase, further confirming their neurogenic potential (Fig. 2C). Together, tNSCs expressed a typical pattern of early neuroectodermal and/or NSC marker genes during the expansion phase in vitro, including major factors for proliferation and self-renewal as well as neurogenic differentiation, such as proneural genes and Pax6.

Further evidence for the stem cell–like nature of tNSCs within the neurospheres is the demonstration of clonogenicity of individual cells in the single-cell culture assay showing the potential of clonally derived neurospheres to differentiate into both neurons and astrocytes. In addition, these results demonstrate that neurons and glia are de novo–generated from proliferating cells (Fig. 3C, 3D). Finally, showing proliferation by PI-FACS analysis, BrdU labeling and Ki67 immunostaining as well as the expression of telomerase [54], these tNSCs fulfill the major characteristics of multipotent NSCs. After removal of mitogens, plating the cells onto PLL, and incubation with BDNF, db-cAMP, and retinoic acid for 14 days, tNSCs differentiate into all major cell types of the CNS, namely mature ($MAP2ab^+$) neurons, oligodendrocytes, and astrocytes with an approximate ratio of 1:1.5:14, respectively. Replacement of the mentioned growth factors with various combinations of growth factors and/or cytokines did not lead to major changes of this differentiation capacity (Table 1). In the presence of selected growth factors (see Materials and Methods for details), tNSCs differentiated into cells expressing the markers for cholinergic, GABAergic, or glutamatergic neurons with similar amounts of the distinct neuronal subpopulations with respect to the various differentiation protocols. Thus, differentiation of tNSCs into these neuronal subtypes did not depend on pre-stimulation with FGF-8 and Shh or co-culture with feeder cells such as MEFs, astrocytes, or PA6 cells (Fig. 4B). Interestingly, no serotoninergic cells could be observed with any differentiation protocol tested.

We further demonstrated that a high percentage of differentiated adult tNSCs acquired functional properties of nerve cells, such as generation of TTX-sensitive sodium channels and action potentials similar to differentiated fetal mouse mesencephalic NSCs [38] or adult NSCs derived from mouse SVZ [75]. A subset of these cells expressed currents with the characteristics of functional $GABA_A$ receptors as well as ionotropic glutamate receptors, including the NMDA-subtype known to be expressed exclusively by neuronal cells [56]. Together, this in vitro differentiation capacity of tNSCs is similar to that of NSCs derived from fetal brain as well as the principal neurogenic regions (hippocampus and SVZ of the lateral ventricles) of the adult brain of various species [21, 31, 41, 76–78]. Zhao and colleagues demonstrated neurogenesis in the adult substantia nigra of C57BL/6 mice in vivo [7]. Two other studies did not find newly born neurons in the adult substantia nigra of normal or lesioned rodents [13, 16]. Moreover, Lie and colleagues found the production of glial cells, but not of neuronal cells, from adult substantia nigra progenitor cells in vivo [16]. In contrast, the in vitro differentiation capacity of these substantia nigra NSCs seems to include neuronal cell lineages [16]. However, this study reported only differentiation into immature neurons ($NeuN^+$ or $Tuj1^+$ cells) and did not show any functionality or neuron subtype specification [16].

The analysis of neuronal subtype differentiation of tNSCs revealed that without pre-stimulating the cells with FGF-8 and Shh and subsequent co-culture with PA6 stromal cells, no TH^+ dopaminergic neurons could be achieved. However, after a multistep differentiation protocol using pre-stimulation and subsequent co-culture of tNSCs with PA6 cells, a small subset of cells not only acquired typical morphological features of dopaminergic cells but also produced the neurotransmitter dopamine, demonstrating the differentiation of tNSCs into functional dopaminergic neurons (Figs. 4, 7). No dopaminergic neurogenesis was detected using other cell types for feeder layer cultures, such as cortical or striatal astrocytes known to induce neuro-

genesis in adult NSCs [78] or MEFs, normally used for proliferation of ESCs. These data suggest a crucial role of PA6 cells (or the so-called stromal cell–derived inducing activity [30]) on dopaminergic neurogenesis not only for ESCs but also for adult tNSCs. However, in contrast to ESCs, tNSCs seem to need an additional priming step to become dopaminergic, such as the pre-incubation procedure with FGF-8 and Shh used in the present study.

Zhao and colleagues demonstrated dopaminergic neurogenesis in the adult substantia nigra of C57BL/6 mice in vivo [7]. A subsequent study was not able to reproduce these results or demonstrate newly generated dopaminergic neurons by the BrdU incorporation assay in normal or 6-hydroxydopamine–lesioned animals [13]. In contrast to the latter results established in vivo, we were able to show dopaminergic specification of isolated adult tNSCs in vitro. This fact is in contrast to previous results on adult NSCs not reporting dopaminergic specification of adult NSCs in vitro independent of the region of origin of the NSCs [7, 13, 16, 78]. The reasons for these discrepancies are likely the following: (a) The in vivo differentiation capacity may not reflect the entire lineage potential of resident progenitor cells, because regional environmental factors appear to restrict in situ differentiation to distinct neural lineages [16–18]. We established a multistep differentiation protocol including coculturing the tNSCs with PA6 stromal cells known to have potent effects on dopaminergic differentiation of ESCs in vitro [30] to provide an environment sufficient for dopaminergic specification in vitro of isolated and long-term expanded adult tNSCs. However, the amounts of dopaminergic neurons generated from adult tNSCs are very low (≈2.5% of all neurons or ≈0.25% of all cells, which is five- to 10-fold less than differentiated fetal mesencephalic NSCs derived from rodents or humans) [29, 38, 79]. The knowledge of the specific factors produced by PA6 stromal cells, which induce dopaminergic specification, will help to further optimize the efficiency of dopaminergic specification of adult NSCs. High yields of dopaminergic cells would be essential for characterization of the intracellular mechanisms of adult dopaminergic neurogenesis as well as the NSC-derived dopaminergic neurons. (b) We used, for the first time, NSCs from the whole adult tegmentum and not just from the substantia nigra or the principal neurogenic regions of the adult brain [7, 16, 78]. Future studies are warranted to further define the exact region within the adult tegmentum from which "pre-dopaminergic" NSCs can be generated.

SUMMARY

We demonstrated the presence of multipotent clonogenic NSCs in the tegmentum of adult mice with the differentiation capacity similar to embryonic/fetal mesencephalic NSCs, including specification into functional nerve cells such as dopaminergic and GABAergic neurons. Previous reports suggest that these cells were derived from the SVZ of the aqueduct and/or fourth ventricle, a structure that is nearby the substantia nigra pars compacta (A9 region) where the degenerating dopaminergic neurons in Parkinson's disease (PD) are located. Recent studies failed to conclusively demonstrate dopaminergic neurogenesis in the adult mammalian midbrain in vivo [7, 13, 16, 80], but our results suggest that NSCs residing in the adult midbrain/hindbrain area can give rise to new functional (dopaminergic) neurons when exposed to appropriate environmental signals. The presented developmental potential of adult tNSCs is one prerequisite for potential future endogenous cell replacement strategies in PD. However, future studies are warranted to clarify the mechanisms for controlling proliferation and dopaminergic differentiation of these adult tNSCs. The presented novel cell culture system provides a powerful tool for investigating these molecular mechanisms of adult neurogenesis and dopaminergic differentiation.

ACKNOWLEDGMENTS

We thank Oana M. Popa, Snezana Maljevic, and Holger Lerche for fruitful discussions; and Thomas Lenk for technical assistance. This work was supported in part by grants from the Interdisciplinary Center for Clinical Research Ulm (Interdiszlplinäres Zentrum für Klinische Forschung [IZKF] Ulm [Project D6] to A.S. and the German Federal Ministry of Education and Research (Bundesministerium für Bildung und Forschung [BMBF]; Polish-German Cooperation in Neuroscience Program) to A.S. A.H. was supported by an IZKF fellowship as a member of the graduate college GRK460, Ulm.

DISCLOSURES

The authors indicate no potential conflicts of interest.

REFERENCES

1 Altman J, Das GD. Autoradiographic and histological evidence of postnatal hippocampal neurogenesis in rats. J Comp Neurol 1965;124:319–335.

2 Gould E, Reeves AJ, Graziano MS et al. Neurogenesis in the neocortex of adult primates. Science 1999;286:548–552.

3 Lois C, Alvarez-Buylla A. Proliferating subventricular zone cells in the adult mammalian forebrain can differentiate into neurons and glia. Proc Natl Acad Sci U S A 1993;90:2074–2077.

4 Levison SW, Goldman JE. Both oligodendrocytes and astrocytes develop from progenitors in the subventricular zone of postnatal rat forebrain. Neuron 1993;10:201–212.

5 Kuhn HG, Dickinson-Anson H, Gage FH. Neurogenesis in the dentate gyrus of the adult rat: Age-related decrease of neuronal progenitor proliferation. J Neurosci 1996;16:2027–2033.

6 Bernier PJ, Bedard A, Vinet J et al. Newly generated neurons in the amygdala and adjoining cortex of adult primates. Proc Natl Acad Sci U S A 2002;99:11464–11469.

7 Zhao M, Momma S, Delfani K et al. Evidence for neurogenesis in the adult mammalian substantia nigra. Proc Natl Acad Sci U S A 2003;100:7925–7930.

8 Jin K, Sun Y, Xie L et al. Directed migration of neuronal precursors into the ischemic cerebral cortex and striatum. Mol Cell Neurosci 2003;24:171–189.

9 Magavi SS, Leavitt BR, Macklis JD. Induction of neurogenesis in the neocortex of adult mice. Nature 2000;405:951–955.

10 Jiang W, Gu W, Brannstrom T et al. Cortical neurogenesis in adult rats after transient middle cerebral artery occlusion. Stroke 2001;32:1201–1207.

11 Koketsu D, Mikami A, Miyamoto Y et al. Nonrenewal of neurons in the cerebral neocortex of adult macaque monkeys. J Neurosci 2003;23:937–942.

12 Kornack DR, Rakic P. Cell proliferation without neurogenesis in adult primate neocortex. Science Dec 7 2001;294:2127–2130.

13 Frielingsdorf H, Schwarz K, Brundin P et al. No evidence for new dopaminergic neurons in the adult mammalian substantia nigra. Proc Natl Acad Sci U S A 2004;101:10177–10182.

14 Rakic P. Adult neurogenesis in mammals: An identity crisis. J Neurosci 2002;22:614–618.

15 Gould E, Gross CG. Neurogenesis in adult mammals: Some progress and problems. J Neurosci 2002;22:619–623.

16 Lie DC, Dziewczapolski G, Willhoite AR et al. The adult substantia nigra contains progenitor cells with neurogenic potential. J Neurosci 2002;22:6639–6649.

17 Shihabuddin LS, Horner PJ, Ray J et al. Adult spinal cord stem cells generate neurons after transplantation in the adult dentate gyrus. J Neurosci 2000;20:8727–8735.

18 Weiss S, Dunne C, Hewson J et al. Multipotent CNS stem cells are present in the adult mammalian spinal cord and ventricular neuroaxis. J Neurosci 1996;16:7599–7609.

19 Palmer TD, Markakis EA, Willhoite AR et al. Fibroblast growth factor-2 activates a latent neurogenic program in neural stem cells from diverse regions of the adult CNS. J Neurosci 1999;19:8487–8497.

20 Rietze RL, Valcanis H, Brooker GF et al. Purification of a pluripotent neural stem cell from the adult mouse brain. Nature 2001;412:736–739.

21 Reynolds BA, Weiss S. Generation of neurons and astrocytes from isolated cells of the adult mammalian central nervous system. Science 1992;255:1707–1710.

22 Doetsch F, Petreanu L, Caille I et al. EGF converts transit-amplifying neurogenic precursors in the adult brain into multipotent stem cells. Neuron 2002;36:1021–1034.

23 Hack MA, Sugimori M, Lundberg C et al. Regionalization and fate specification in neurospheres: The role of Olig2 and Pax6. Mol Cell Neurosci 2004;25:664–678.

24 Johansson CB, Momma S, Clarke DL et al. Identification of a neural stem cell in the adult mammalian central nervous system. Cell 1999;96:25–34.

25 Alvarez-Buylla A, Seri B, Doetsch F. Identification of neural stem cells in the adult vertebrate brain. Brain Res Bull 2002;57:751–758.

26 Gritti A, Frolichsthal-Schoeller P, Galli R et al. Epidermal and fibroblast growth factors behave as mitogenic regulators for a single multipotent stem cell-like population from the subventricular region of the adult mouse forebrain. J Neurosci 1999;19:3287–3297.

27 Gritti A, Cova L, Parati EA et al. Basic fibroblast growth factor supports the proliferation of epidermal growth factor-generated neuronal precursor cells of the adult mouse CNS. Neurosci Lett 1995;185:151–154.

28 Doetsch F. The glial identity of neural stem cells. Nat Neurosci 2003;6:1127–1134.

29 Storch A, Paul G, Csete M et al. Long-term proliferation and dopaminergic differentiation of human mesencephalic neural precursor cells. Exp Neurol 2001;170:317–325.

30 Kawasaki H, Mizuseki K, Nishikawa S et al. Induction of midbrain dopaminergic neurons from ES cells by stromal cell-derived inducing activity. Neuron 2000;28:31–40.

31 Uchida N, Buck DW, He D et al. Direct isolation of human central nervous system stem cells. Proc Natl Acad Sci U S A 2000;97:14720–14725.

32 Milosevic J, Storch A, Schwarz J. Cryopreservation does not affect proliferation and pluripotency of murine neural stem cells. STEM CELLS 2005;23:681–688.

33 Takebayashi H, Yoshida S, Sugimori M et al. Dynamic expression of basic helix-loop-helix Olig family members: Implication of Olig2 in neuron and oligodendrocyte differentiation and identification of a new member, Olig3. Mech Dev 2000 99:143–148.

34 Emrich T, Karl G. Nonradioactive detection of telomerase activity using a PCR-ELISA-based telomeric repeat amplification protocol. Methods Mol Biol 2002;191:147–158.

35 Saldanha SN, Andrews LG, Tollefsbol TO. Analysis of telomerase activity and detection of its catalytic subunit, hTERT. Anal Biochem 2003;315:1–21.

36 Chung S, Sonntag KC, Andersson T et al. Genetic engineering of mouse embryonic stem cells by Nurr1 enhances differentiation and maturation into dopaminergic neurons. Eur J Neurosci 2002;16:1829–1838.

37 Milosevic J, Schwarz SC, Krohn K et al. Low atmospheric oxygen avoids maturation, senescence and cell death of murine mesencephalic neural precursors. J Neurochem 2005;92:718–729.

38 Storch A, Lester HA, Boehm BO et al. Functional characterization of dopaminergic neurons derived from rodent mesencephalic progenitor cells. J Chem Neuroanat 2003;26:133–142.

39 Hermann A, Gastl R, Liebau S et al. Efficient generation of neural stem cell-like cells from adult human bone marrow stromal cells. J Cell Sci 2004;117:4411–4422.

40 Gerlach M, Gsell W, Kornhuber J et al. A post mortem study on neurochemical markers of dopaminergic, GABA-ergic and glutamatergic neurons in basal ganglia-thalamocortical circuits in Parkinson syndrome. Brain Res 1996;741:142–152.

41 Cattaneo E, McKay R. Proliferation and differentiation of neuronal stem cells regulated by nerve growth factor. Nature 1990;347:762–765.

42 Kaneko Y, Sakakibara S, Imai T et al. Musashi1: An evolutionally conserved marker for CNS progenitor cells including neural stem cells. Dev Neurosci 2000;22:139–153.

43 Bylund M, Andersson E, Novitch BG et al. Vertebrate neurogenesis is counteracted by Sox1–3 activity. Nat Neurosci 2003;6:1162–1168.

44 Graham V, Khudyakov J, Ellis P et al. SOX2 functions to maintain neural progenitor identity. Neuron 2003;39:749–765.

45 Bertrand N, Castro DS, Guillemot F. Proneural genes and the specification of neural cell types. Nat Rev Neurosci 2002;3:517–530.

46 Simmons AD, Horton S, Abney AL et al. Neurogenin2 expression in ventral and dorsal spinal neural tube progenitor cells is regulated by distinct enhancers. Dev Biol 2001;229:327–339.

47 Nieto M, Schuurmans C, Britz O et al. Neural bHLH genes control the neuronal versus glial fate decision in cortical progenitors. Neuron 2001;29:401–413.

48 Franklin A, Kao A, Tapscott S et al. NeuroD homologue expression during cortical development in the human brain. J Child Neurol 2001;16:849–853.

49 Key G, Kubbutat MH, Gerdes J. Assessment of cell proliferation by means of an enzyme-linked immunosorbent assay based on the detection of the Ki-67 protein. J Immunol Methods 1994;177:113–117.

50 Gerdes J, Lemke H, Baisch H et al. Cell cycle analysis of a cell proliferation-associated human nuclear antigen defined by the monoclonal antibody Ki-67. J Immunol 1984;133:1710–1715.

51 Gerdes J, Schwab U, Lemke H et al. Production of a mouse monoclonal antibody reactive with a human nuclear antigen associated with cell proliferation. Int J Cancer 1983;31:13–20.

52 Ostenfeld T, Caldwell MA, Prowse KR et al. Human neural precursor cells express low levels of telomerase in vitro and show diminishing cell proliferation with extensive axonal outgrowth following transplantation. Exp Neurol 2000;164:215–226.

53 Meyerson M, Counter CM, Eaton EN et al. hEST2, the putative human telomerase catalytic subunit gene, is up-regulated in tumor cells and during immortalization. Cell 1997;90:785–795.

54 Mattson MP, Klapper W. Emerging roles for telomerase in neuronal development and apoptosis. J Neurosci Res 2001;63:1–9.

55 Milosevic J, Storch A, Schwarz J. Spontaneous apoptosis in murine free-floating neurospheres. Exp Cell Res 2004;294:9–17.

56 Verkhratsky A, Steinhauser C. Ion channels in glial cells. Brain Res Brain Res Rev 32:380–412, 2000.

57 Yan J, Studer L, McKay RD. Ascorbic acid increases the yield of dopaminergic neurons derived from basic fibroblast growth factor expanded mesencephalic precursors. J Neurochem 2001;76:307–311.

58 Studer L, Csete M, Lee SH et al. Enhanced proliferation, survival, and dopaminergic differentiation of CNS precursors in lowered oxygen. J Neurosci 2000;20:7377–7383.

59 Murayama A, Matsuzaki Y, Kawaguchi A et al. Flow cytometric analysis of neural stem cells in the developing and adult mouse brain. J Neurosci Res 2002;69:837–847.

60 Studer L, Tabar V, McKay RD. Transplantation of expanded mesencephalic precursors leads to recovery in parkinsonian rats. Nat Neurosci 1998;1:290–295.

61 Lendahl U, Zimmerman LB, McKay RD. CNS stem cells express a new class of intermediate filament protein. Cell 1990;60:585–595.

62 Dahlstrand J, Lardelli M, Lendahl U. Nestin mRNA expression correlates with the central nervous system progenitor cell state in many, but not all, regions of developing central nervous system. Brain Res Dev Brain Res 1995;84:109–129.

63 Hockfield S, McKay RD. Identification of major cell classes in the developing mammalian nervous system. J Neurosci 1985;5:3310–3328.

64 Frederiksen K, McKay RD. Proliferation and differentiation of rat neuroepithelial precursor cells in vivo. J Neurosci 1988;8:1144–1151.

65 Palmer TD, Willhoite AR, Gage FH. Vascular niche for adult hippocampal neurogenesis. J Comp Neurol 2000;425:479–494.

66 Blumcke I, Schewe JC, Normann S et al. Increase of nestin-immunoreactive neural precursor cells in the dentate gyrus of pediatric patients with early-onset temporal lobe epilepsy. Hippocampus 2001;11:311–321.

67 Nacher J, Rosell DR, Alonso-Llosa G et al. NMDA receptor antagonist treatment induces a long-lasting increase in the number of proliferating cells, PSA-NCAM-immunoreactive granule neurons and radial glia in the adult rat dentate gyrus. Eur J Neurosci 2001;13:512–520.

68 Gangemi RM, Perera M, Corte G. Regulatory genes controlling cell fate choice in embryonic and adult neural stem cells. J Neurochem 2004;89:286–306.

69 Ross SE, Greenberg ME, Stiles CD. Basic helix-loop-helix factors in cortical development. Neuron 2003;39:13–25.

70 Fode C, Ma Q, Casarosa S et al. A role for neural determination genes in specifying the dorsoventral identity of telencephalic neurons. Genes Dev 2000;14:67–80.

71 Zhou Q, Anderson DJ. The bHLH transcription factors OLIG2 and OLIG1 couple neuronal and glial subtype specification. Cell 2002;109:61–73.

72 Heins N, Malatesta P, Cecconi F et al. Glial cells generate neurons: The role of the transcription factor Pax6. Nat Neurosci 2002;5:308–315.

73 Hartfuss E, Galli R, Heins N et al. Characterization of CNS precursor subtypes and radial glia. Dev Biol 2001;229:15–30.

74 Alvarez-Buylla A, Garcia-Verdugo JM, Tramontin AD. A unified hypothesis on the lineage of neural stem cells. Nat Rev Neurosci 2001;2:287–293.

75 Liu RH, Morassutti DJ, Whittemore SR et al. Electrophysiological properties of mitogen-expanded adult rat spinal cord and subventricular zone neural precursor cells. Exp Neurol 1999;158:143–154.

76 Carvey PM, Ling ZD, Sortwell CE et al. A clonal line of mesencephalic progenitor cells converted to dopamine neurons by hematopoietic cytokines: A source of cells for transplantation in Parkinson's disease. Exp Neurol 2001;171:98–108.

77 Kilpatrick TJ, Bartlett PF. Cloning and growth of multipotential neural precursors: Requirements for proliferation and differentiation. Neuron 1993;10:255–265.

78 Song H, Stevens CF, Gage FH. Astroglia induce neurogenesis from adult neural stem cells. Nature 2002;417:39–44.

79 Ling ZD, Potter ED, Lipton JW et al. Differentiation of mesencephalic progenitor cells into dopaminergic neurons by cytokines. Exp Neurol 1998;149:411–423.

80 Kay JN, Blum M. Differential response of ventral midbrain and striatal progenitor cells to lesions of the nigrostriatal dopaminergic projection. Dev Neurosci 2000;22:56–67.